Pergamon

Int. J. Heat Mass Transfer. Vol. 40, No. 18, pp. 4329–4335, 1997

Printed in Great Britain
0017-9310/97 $17.00+0.00

PII: S0017-9310(97)00081-1

Natural convection heat transfer from an isothermal vertical surface to a fluid saturated thermally stratified porous medium

D. ANGIRASA and G. P. PETERSON†

Department of Mechanical Engineering, Texas A & M University,
301 Weisenbaker Engineering Research Center, College Station, TX 77843-3126, U.S.A.

(*Received* 14 *June* 1996 *and in final form* 25 *February* 1997)

Abstract—Presented here are the results of a numerical study of natural convection heat transfer in a stably stratified, fluid saturated low porosity medium, in which Darcy flow prevails. In this investigation, the boundary layer approximations are discarded and a wide range of ambient thermal stratification levels is considered. The results indicate that the ambient thermal stratification has a significant effect on the flow and temperature fields, and that this effect differs considerably at higher levels of stratification. The flow reversal and temperature defects are significantly smaller in the porous media than in a viscous fluid, due to the stabilization of the flow by the solid matrix. To generalize the result, the Nusselt number data are correlated with the thermal stratification parameter to yield a functional relationship. © 1997 Elsevier Science Ltd.

1. INTRODUCTION

Buoyancy-driven convection in a fluid saturated, density-stratified porous medium has applications in a wide range of areas including geothermal fields and nuclear-waste deposits. In the current study, the thermal and fluid transport adjacent to a vertical surface embedded in a stable, thermally stratified saturated porous medium is investigated, with particular attention given to how the thermal stratification affects the convection heat transfer.

The fundamental nature of natural convection flows in isothermal porous media is well-documented in the literature [1] and a number of boundary layer studies of convection heat transfer from surfaces to a thermally stratified porous ambient medium have also been reported. In an early study, Johnson and Cheng [2] considered different wall and boundary conditions, and found that similarity is not possible for the case of an isothermal surface in a stably stratified medium. This had been shown to be true earlier for natural convection in a stably stratified viscous fluid [3]. More recently, approximate integral solutions for the porous media problem have been presented by Bejan [4], Nakayama and Koyama [5], and Singh and Sharma [6].

Similarity solutions for convection heat transfer in porous media, where both the wall and ambient temperatures increase with height, have been developed by Nakayama and Koyama [7], and Takhar and Pop [8], and series and local nonsimilarity solutions have been presented by Lai *et al.* [9]. For the case of buoyancy-induced flow over an isothermal curved surface in a thermally stratified porous medium, where both the surface and ambient temperatures increase with the height, Nakayama and Koyama [10] utilized similarity methods, while other investigators [12] provided approximate analytical solutions based on an earlier study of the Falkner–Skan equation [11]. Other approaches include series solutions [13], the application of perturbation methods for the case of non-Darcy flows [14] and numerical solutions that consider convective, boundary and inertia effects for boundary layer flows [15].

Boundary layer analyses have been shown to be inaccurate for natural convection flows in stratified fluids, especially for large stratification levels, i.e. steep increases in the ambient temperature with respect to height [16]. The results of this investigation indicate that it is desirable to solve the complete equations in order to obtain accurate solutions and to understand the physical mechanisms that govern these flows. For this reason, in the current investigation complete numerical solutions are presented for Darcy flows in linear, stably-stratified fluid saturated porous media. A wide range of ambient stratification levels is considered. The flow and thermal fields as well as Nusselt number data are given and the fundamental physical processes of these complex flows and thermal transport are examined.

2. ANALYSIS

The physical configuration and the coordinate system are shown in Fig. 1, where a vertical surface of height L is embedded in a fluid saturated porous

† Author to whom correspondence should be addressed.

NOMENCLATURE

g	gravitational acceleration
$\bar{h}$	average heat transfer coefficient
k_0	thermal conductivity of the stagnant medium
K	permeability
L	height of the surface
Nu	average Nusselt number
p	dynamic pressure
Ra	Rayleigh number $= g\beta\Delta tKL/\nu\alpha$
t	temperature
T	nondimensional temperature
u, v	velocity components
U, V	nondimensional velocity components
V_c	convective velocity $= g\beta\Delta tK/\nu$
x, y	space coordinates
X, Y	nondimensional space coordinates.

Greek symbols

α	thermal diffusivity $= k_0/(\rho C)_f$
β	coefficient of thermal expansion $= -1/\rho\ (\partial\rho/\partial t)_p$
ν	kinematic viscosity
ρ	density of the fluid
σ	ratio of heat capacities of the stagnant medium and the fluid $= (\rho C)_0/(\rho C)_f$
τ	time
τ^*	nondimensional time
ψ	stream function
ω	vorticity.

Subscripts

f	fluid
w	wall
0	stagnant medium
∞	reference.

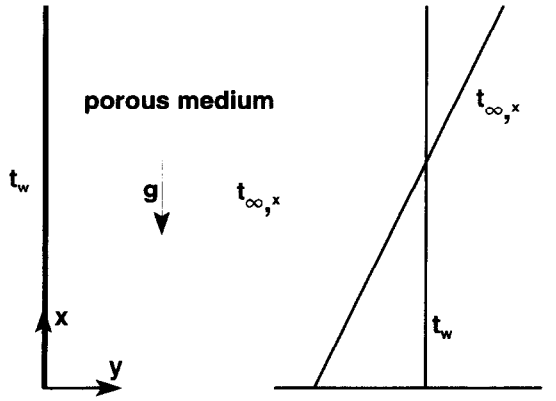

Fig. 1. Geometry and coordinate system.

medium. The temperature of the vertical surface is t_w, and the ambient temperature, $t_{\infty,x}$, increases linearly with respect to x, beginning with $t_{\infty,0}$ at $x = 0$. The buoyancy-driven Darcy flow and transport adjacent to the vertical surface can be described by the following two-dimensional equations in nondimensional form:

$$\frac{\partial U}{\partial X} + \frac{\partial V}{\partial Y} = 0 \tag{1}$$

$$\frac{\partial U}{\partial Y} - \frac{\partial V}{\partial X} = \frac{\partial T}{\partial Y} \tag{2}$$

$$\sigma\frac{\partial T}{\partial \tau^*} + U\frac{\partial T}{\partial X} + V\frac{\partial T}{\partial Y} + SU = \frac{1}{Ra}\left(\frac{\partial^2 T}{\partial X^2} + \frac{\partial^2 T}{\partial Y^2}\right) \tag{3}$$

where σ is the ratio of heat capacities of the stagnant medium and the fluid.

Two other parameters which appear in the nondimensional conservation equations are the Rayleigh number, $Ra = g\beta\Delta tKL/\nu\alpha$ and the thermal stratification parameter, S, defined as:

$$S = \frac{1}{\Delta t}\frac{\mathrm{d}t_{\infty,x}}{\mathrm{d}X}. \tag{4}$$

Here, K is the permeability, g is the gravitational acceleration, α is the thermal diffusivity given by $\alpha = k_0/(\rho C)_f$ and ν is the kinematic viscosity. The temperature potential, Δt is given by $(t_w - t_{\infty,0})$. The following nondimensional variables were defined in arriving at equations (1)–(4).

$$X = \frac{x}{L},\ Y = \frac{y}{L},\ \tau^* = \frac{\tau V_c}{L},\ U = \frac{u}{V_c},$$

$$V = \frac{v}{V_c} \quad \text{and} \quad T = \frac{(t - t_{\infty,x})}{(t_w - t_{\infty,0})} \tag{5}$$

where V_c is a convective velocity given by $V_c = g\beta\Delta tK/\nu$. The nondimensional boundary conditions are:

$$Y = 0: \quad V = 0,\ T = 1 - SX \quad \text{and}$$

$$Y \to \infty \quad U = 0,\ T = 0. \tag{6}$$

The wall temperature condition, in nondimensional form, can be obtained as:

$$T_w = \frac{(t_w - t_{\infty,x})}{(t_w - t_{\infty,0})} = 1 - \frac{(t_{\infty,x} - t_{\infty,0})}{\Delta t_0} = 1 - SX. \tag{7}$$

Defining the nondimensional vorticity as:

$$\omega = \frac{\partial U}{\partial Y} - \frac{\partial V}{\partial X} \tag{8}$$

allows equation (2) to be written as

$$\omega = \frac{\partial T}{\partial Y}. \tag{9}$$

Although vorticity is not a variable of interest here, it is still defined for convenience, because the left-hand side of equation (2) has the appearance of vorticity. The nondimensional stream function, ψ, is defined such that:

$$U = \frac{\partial \psi}{\partial Y} \quad \text{and} \quad V = -\frac{\partial \psi}{\partial X}. \tag{10}$$

Combining equations (8) and (10), the stream function equation can be expressed as:

$$\frac{\partial^2 \psi}{\partial X^2} + \frac{\partial^2 \psi}{\partial Y^2} = \omega. \tag{11}$$

Finally, the average Nusselt number is defined as:

$$Nu = \frac{\bar{h}L}{k_0} = \int_0^1 \left(-\frac{\partial T}{\partial Y} \right)_{Y=0} \mathrm{d}X \tag{12}$$

where $\bar{h}$ is the average heat transfer coefficient.

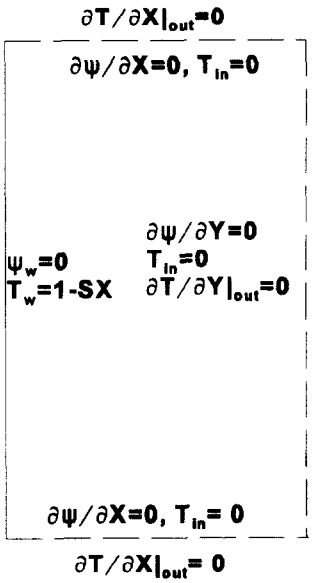

Fig. 2. Numerical boundary conditions.

3. NUMERICAL METHODS

The energy equation is solved using the alternating direction implicit scheme (ADI) of Peaceman and Rachford described by Roache [17]. The convective terms were discretized with upwind differencing and the diffusion terms with central differencing. The unsteady energy conservation equation is then marched in time to an asymptotic, steady-state solution. Vorticity is evaluated from equation (9) using a central difference formulation. The stream function equation, equation (11) was iteratively solved within each time-step by the successive over relaxation (SOR) method. It should be noted that in the current problem, the wall vorticities are not required to obtain the vorticity field and the wall vorticity equals the local Nusselt number. The vorticity could be evaluated using the field solution of T through equation (9). The average Nusselt number was calculated by the numerical integration of equation (12) using an open-ended formulation of Simpson's rule [18].

The initial conditions for marching the discretized equation given in equation (3) are:

$$\tau^* = 0 \quad T = 0, U = 0, V = 0 \quad \text{for all } X \text{ and } Y \tag{13}$$

and the boundary conditions for equations (3) and (11) are shown in Fig. 2. The width of the computational domain was conservatively estimated from the similarity solution for $S = 0$ [19] and fixed by a trial and error process.

An absolute error criterion with a value of less than 10^{-5} was used to ensure that the solution had reached a steady-state solution. Constant grid spacings were employed in each direction and the number of grid points in each direction was varied to make the grid dependent error less than 1% in each of the field variables. The number of grid points employed was 81×101, which yields a maximum error of 2.5% in the Nusselt number at its asymptotic value. The calculations were time consuming and typically 40 000 time-steps were required to reach a steady-state solution. A time-step of 0.001 was chosen after checking that this value had no impact on the steady-state solution.

4. RESULTS AND DISCUSSION

When the ambient conditions are isothermal, the numerical value of S is zero. If the ambient temperature, $t_{\infty,x}$, equals the surface temperature, t_w, at $X = 1$, then $S = 1$. Between these two limits of S, the wall temperature at X is necessarily larger than the ambient temperature. When $S > 1$, a portion of the surface at the top falls below the ambient temperature, resulting in a downward flow in this region. The upward and downward flow meet at a location where the temperature potential, Δt_x vanishes and together emerge as a horizontal plume. For $S = 2$, the plume location is at the mid-height of the surface. In the previous studies surveyed in the introduction, this interesting phenomena of plume behavior and its effect on heat transfer were not considered. If the ratio of the heat capacities, σ, has a value of less than unity, it has no influence on the steady-state solutions and, hence, in the current investigation this value is assumed to be unity.

The numerical results obtained in this investigation were first compared with two previous analytical studies in terms of the vertical natural convection boundary layers. In Table 1, Nusselt number data are compared with the similarity solution of Cheng and Minkowycz [19] for $S = 0$. In Table 2, the numerically obtained Nusselt number data are compared with the

Table 1. Average Nusselt number, Nu_0

	$Ra = 10^3$	5×10^3	10^4
Present	27.93	61.70	86.26
Cheng and Minkowycz [19]	28.08	62.79	88.8

Table 2. Nu/Nu_0 for all Ra ($S = 0.2$)

Present	0.92
Lai and Kulacki [20]	0.92

local nonsimilarity solution of Lai and Kulacki [20] for $S = 0.2$, which corresponds to a lower level of ambient thermal stratification. In both cases, the numerical results obtained using the method developed herein compare quite favorably with the analytical solutions.

The thermal potential that drives the buoyancy-induced flow in a porous medium decreases with increasing values of the thermal stratification parameter, S. Consequently, as shown in Fig. 3, the vertical velocities diminish. In Fig. 4, the excess temperature profiles (local temperature with the ambient temperature removed) are illustrated for different values of the thermal stratification parameter, S. Here, increasing S spreads the thermal layer farther, while reducing the residual temperature levels. In the viscous fluid flow, the velocity at the wall must be zero to satisfy the no slip condition [16], while in porous media with low porosity, hence low velocity, it is possible to obtain a finite vertical velocity at the wall. This depends on the value of the wall temperature gradient, i.e. equation (2). A further contrast between the flow of viscous fluids and flow through a saturated porous medium is the extent of the flow reversals occurring away from the vertical surface. The reverse velocities in the outer regions of a porous medium are extremely small when compared to viscous flow [16], but are clearly non-zero (Fig. 3).

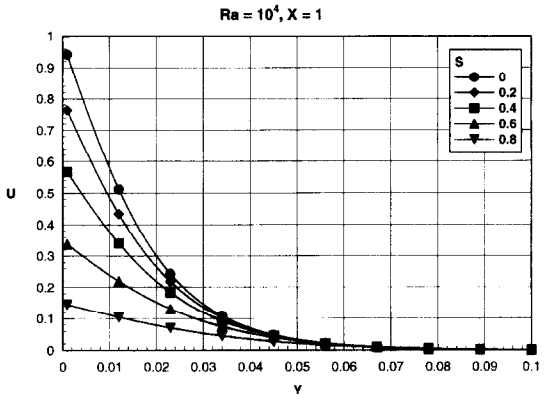

Fig. 3. Effect of thermal stratification on vertical velocity profiles.

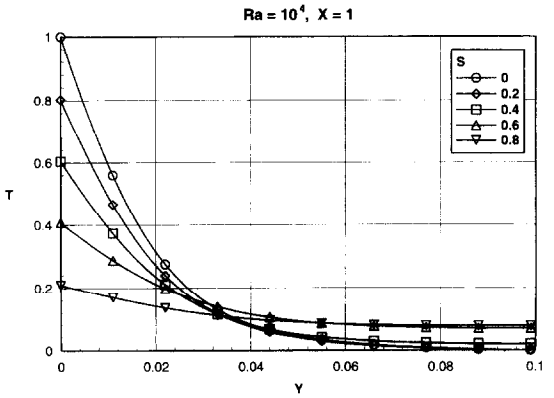

Fig. 4. Effect of thermal stratification on temperature profiles.

Similarly, the temperature defects associated with vertical buoyancy-induced, viscous flows in thermally stratified fluids are very small for flow in a porous medium (Fig. 4). A temperature defect in the outer region occurs because the fluid coming up from below in a thermally stratified environment finds itself in a warmer surroundings, resulting in a 'negative temperature' in the wings of the temperature profiles [16], which leads to the afore-mentioned flow reversal in the outer region of the flow. This phenomenon is well-understood in the context of viscous flows. However, for flow in a porous medium, the presence of a large amount of solid material inhibits the development of temperature defects and the concomitant flow reversal. The solid matrix slows down the flow and redistributes it well, so there is very little temperature defect. While this value is small, it is still non-zero. This has a consequence when a larger value of S (> 1) is considered and a horizontal plume emerges from the vertical wall.

In order to understand the flow field better, particulary at large S, stream function contours are presented in Fig. 5. For $S = 0$, the normal boundary layer structure is easily discerned. As the value of S increases to 0.6, the velocities fall and the flow field spreads farther away from the surface by drawing fluid from the bottom and the lower half of the side. At $S = 1$, the entrainment from the side diminishes and a larger portion of the outflow occurs at the side. One particularly interesting phenomenon of the horizontal plume emanating at $X = 0.5$ for $S = 2$, is illustrated in Fig. 5(d), where the physical mechanism that produces this flow field is more complex.

In the bottom half, the wall temperature is larger than the ambient temperature, while in the top half, the reverse happens. As a result, an upward flow from the bottom leading edge and a downward flow from the top leading edge develop, each over half the length of the surface. These two flows meet at the midpoint ($X = 0.5$) and emerge horizontally as a plume. The location of this plume will be higher if the value of S lies between 1 and 2. The isotherm contours of the residual temperature for the flows under discussion

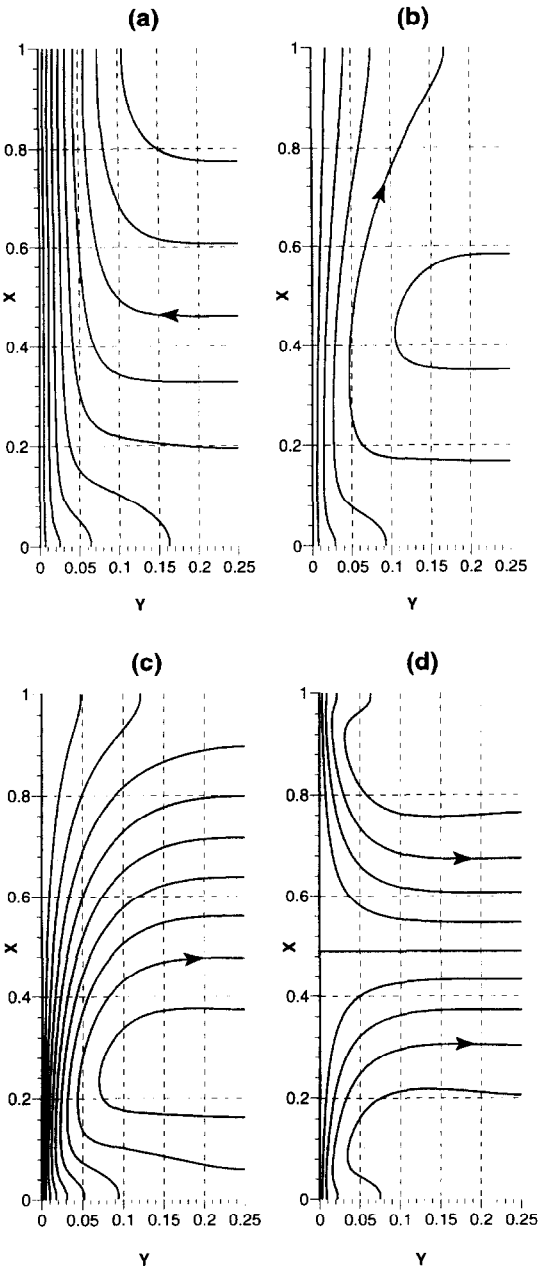

Fig. 5. Stream function contours. S = (a) 0, (b) 0.6, (c) 1 and (d) 2. $\psi_{wall} = 0$, $\Delta\psi$ = (a) 0.005, (b) 0.005, (c) 0.002 and (d) 0.0025.

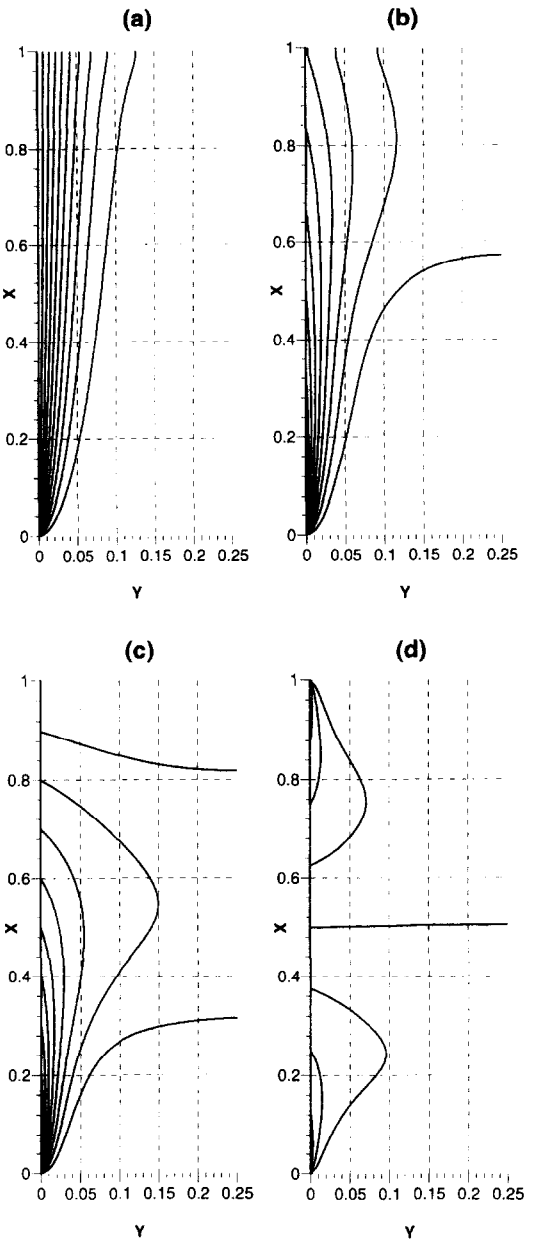

Fig. 6. Isotherm contours of excess temperature. S = (a) 0, (b) 0.6, (c) 1 and (d) 2. $T_{wall} = 1 - SX$, ΔT = (a) 0.1, (b) 0.1, (c) 0.1 and (d) 0.25.

here are illustrated in Fig. 6. As shown, with increasing thermal stratification parameter, the wall temperature gradients fall and the shape of the isotherms confirms the horizontal spreading of the flow at higher values of S. It is interesting to note that in both Figs 5(d) and 6(d), the fields are not symmetric about the horizontal axis at $X = 0.5$.

The previous investigation of Angirasa and Srinivasan [16] explained the physical instabilities occurring in the horizontal plume for a viscous flow as originating in the unequal temperature defects in the two flows, i.e. they have opposite signs. This results in time-dependent flow 'ripples' or 'striations' of an unsteady flow. In a porous medium, however, the magnitude of the temperature defects is very small as was explained above. Consequently, the horizontal plume is not unsteady and no striations are observed, but the very small temperature defects in the upward and downward flows marginally change the symmetry of the flow in the two halves. This asymmetry is time-dependent and periodic. From a numerical point of view, the temperature field in the plume flow does not satisfy the relative error criterion in the solution presented, although absolute convergence is satisfied. The reason for this is clearly the very small magnitude

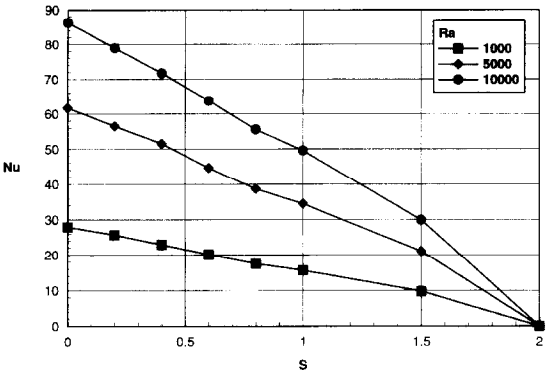

Fig. 7. Nusselt number variation with thermal stratification.

of these instabilities. No attempt is made here to determine numerically the time period for the asymmetry to repeat itself, since the changes are of the same order of magnitude as the numerical errors.

Figure 7 presents the variation of the average Nusselt number as a function of the thermal stratification parameter, S, for Rayleigh numbers of 1000, 5000 and 10000. At any Rayleigh number, the average Nusselt number decreases with increasing S. The Nusselt number is zero when $S = 2$, with the top half of the surface gaining an amount of heat which is equal to the amount lost by the bottom half. For all Rayleigh numbers, the Nu–S variation is linear in the range $0 < S < 1.5$. Hence, in an attempt to obtain a general correlation for the Nusselt number in terms of the thermal stratification parameter, the Nusselt number data are plotted in Fig. 8 as a fraction of Nu_0, the Nusselt number for $S = 0$ for the same Ra. As illustrated, the data collapse on a single line, with a linear variation in the range, $0 < S < 1.5$. The data are correlated by a least-square fit [18] to yield the following expression:

$$\frac{Nu}{Nu_0} = 1 - 0.44\,S \quad 0 \leqslant S \leqslant 1.5. \tag{14}$$

The above correlation is expected to be valid as long as the porosity is low enough that the Darcy flow assumption is justified.

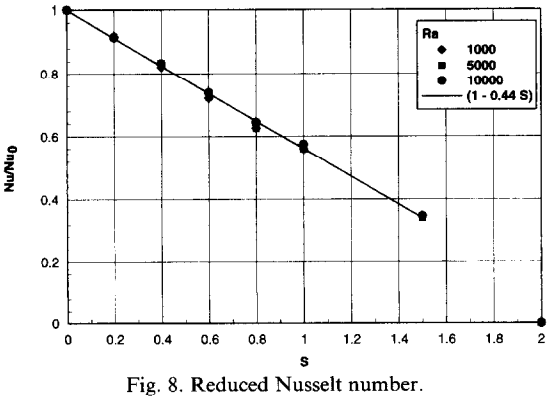

Fig. 8. Reduced Nusselt number.

5. SUMMARY

A numerical study was carried out for natural convection heat transfer from a vertical surface to a stable thermally stratified fluid saturated porous medium. The porosity of the medium was assumed to be small enough that the Darcy flow approximation is valid. However, approximations associated with boundary layer type flow are removed to enable the consideration of a much larger range of thermal stratification levels, where the flow and transport are quite complex. The temperature defects and flow reversal in the outer regions, which have been previously observed in viscous flows, are extremely small for the flow in a porous medium of the type studied here. This can be attributed to the low porosity, where the presence of a large solid matrix stabilizes the flow and effectively redistributes it. The Nusselt number data are correlated to yield a functional relationship between the Nusselt number and thermal stratification parameter.

REFERENCES

1. Cheng, P., Geothermal heat transfer. *Handbook of Heat Transfer Applications*, 2nd edn, eds W. M. Rohsenow, J. P. Hartnett and E. N. Ganic. McGraw-Hill, New York, 1985.
2. Johnson, C. H. and Cheng, P., Possible similarity solutions for free convection boundary layers adjacent to flat plates in porous media. *International Journal of Heat and Mass Transfer*, 1978, **21**, 709–718.
3. Yang, K. T., Novotny, J. L. and Cheng, Y. S., Laminar free convection from a nonisothermal plate immersed in a temperature stratified medium. *International Journal of Heat and Mass Transfer*, 1972, **15**, 1097–1109.
4. Bejan, A., *Convection Heat Transfer*. Wiley, New York, 1984.
5. Nakayama, A. and Koyama, H., An integral method for free convection from a vertical heated surface in a thermally stratified porous medium. *Wärme- und Stoffübertragung*, 1987, **21**, 297–300.
6. Singh, P. and Sharma, K., Integral method to free convection in thermally stratified porous medium. *Acta Mechanica*, 1990, **83**, 157–163.
7. Nakayama, A. and Koyama, H., Effect of thermal stratification on free convection within a porous medium. *AIAA Journal of Thermophysics and Heat Transfer*, 1987, **1**, 282–285.
8. Takhar, H. S. and Pop, I., Free convection from a vertical flat plate to a thermally stratified Darcian fluid. *Mechanics Research Communications*, 1987, **14**, 81–86.
9. Lai, F. C., Pop, I. and Kulacki, F. A., Natural convection from isothermal plates embedded in thermally stratified porous media. *AIAA Journal of Thermophysics and Heat Transfer*, 1990, **4**, 533–535.
10. Nakayama, A. and Koyama, H., Similarity solutions for buoyancy-induced flows over a nonisothermal curved surface in a thermally stratified porous medium. *Applied Scientific Research*, 1989, **46**, 309–322.
11. Dey, J., A simple technique for approximate solutions of the Falkner–Skan equation. *Acta Mechanica*, 1989, 77, 299–305.
12. Govindarajulu, T. and Moorthy, M. B. K., An approximate solution for free convection flows in a thermally stratified porous medium. *Applied Scientific Research*, 1992, **49**, 83–89.
13. Tewari, K. and Singh, P., Natural convection in a thermally stratified fluid saturated porous medium. *Inter-*

national Journal of Engineering Science, 1992, **30,** 1003–1007.

14. Singh, P. and Tewari, K., Non-Darcy free convection from vertical surfaces in thermally stratified porous media. *International Journal of Engineering Science*, 1993, **31,** 1233–1242.
15. Chen, C. K. and Lin, C. R., Natural convection from an isothermal vertical surface embedded in a thermally stratified high-porosity medium. *International Journal of Engineering Science*, 1995, **33,** 131–138.
16. Angirasa, D. and Srinivasan, J., Natural convection heat transfer from an isothermal vertical surface to a stable thermally stratified fluid. *ASME Journal of Heat Transfer*, 1992, **114,** 917–923.
17. Roache, P. J., *Computational Fluid Dynamics*. Hermosa, Albuquerque, NM, 1982.
18. Press, W. H., Flannery, B. P., Teukolsky, S. A. and Vetterling, W. T., *Numerical Recipes: The Art of Scientific Computing*. Cambridge University Press, New York, 1986.
19. Cheng, P. and Minkowycz, W. J., Free convection about a vertical flat plate embedded in a porous medium with application to heat transfer from a dike. *Journal of Geophysical Research*, 1977, **82,** 2040–2044.
20. Lai, F. C. and Kulacki, F. A., Reply by the authors to A. Bejan. *AIAA Journal of Thermophysics and Heat Transfer*, 1992, **6,** 575–576.